

PACS numbers: 61.46.Bc, 61.46.Df, 68.35.-p, 73.22.-f, 81.07.Nb, 82.45.Yz, 82.70.Dd

## Zeta Potential and Degree of the Aggregation of Nanoparticles of the Pyrogenic Silica in the Presence of the Dissolved Metal Chlorides in the Aqueous Medium

L. S. Andriyko, V. I. Zarko, A. I. Marynin\*, V. V. Olishkevskiy\*,  
A. A. Kravchenko, and E. M. Demjanenko

*O. O. Chuiko Institute of Surface Chemistry, N.A.S. of Ukraine,  
17 General Naumov Street,  
03164 Kyiv, Ukraine*

*\*National University of Food Technologies,  
68 Volodymyrska Street,  
01033 Kyiv, Ukraine*

The effects of univalent metals' chlorides (LiCl, NaCl, KCl) at different concentrations (0.001–0.1 M) on the behaviour of nanosilica (0.5–5 wt.%) in aqueous medium are analysed using photon correlation spectroscopy (particle size distribution—PSD) and electrophoresis (zeta potential,  $\zeta$ ). The shift of dissociation constant ( $K_a$ ) estimated for fumed silica hydroxyl sites is observed. Such a change in the  $pK_a$  value is established via quantum-chemical study of the electrolyte–silica surface interaction. The correlation dependence associated with  $pK_a$ , an effective diameter, and  $\zeta$ -potential of silica nanoparticles is demonstrated.

Методом фотон-кореляційної спектроскопії досліджено вплив концентрації (0,001–0,1 М) хлоридів лужних металів (LiCl, NaCl, KCl) на ступінь агрегації та дзета-потенціал частинок пірогенного кремнезему (0,5–5% мас.) у водному середовищі. На основі результатів квантово-хімічного моделювання взаємодії розчинів електролітів із поверхнею кремнезему проведено оцінювання величини зсуву константи дисоціації ( $pK_a$ ) силанольних груп поверхні у присутності гідратованих йонів таких солей. Показано кореляційну залежність між цією величиною, значеннями ефективного діаметра та дзета-потенціалом наночастинок кремнезему, що досліджувався у зазначених розчинах.

Методом фотон-корреляционной спектроскопии исследовано влияние концентрации (0,001–0,1 М) хлоридов щелочных металлов (LiCl, NaCl, KCl) на степень агрегации и дзета-потенциал частиц пиrogenного кремнезёма (0,5–5 масс.%) в водной среде. На основании результатов

квантово-химического моделирования взаимодействия растворов электролитов с поверхностью кремнезёма оценены величины сдвига константы диссоциации ( $pK_a$ ) силанольных групп поверхности в присутствии гидратированных ионов таких солей. Показана корреляционная зависимость между этой величиной, значениями эффективного диаметра и дзета-потенциала наночастиц исследуемого кремнезёма в указанных растворах.

**Key words:** nanosilica, metal chlorides, aqueous suspension, particle size distribution, zeta potential.

**Ключові слова:** нанокремнезем, хлориди металів, водні суспензії, розподіл частинок за розмірами, дзета-потенціал.

**Ключевые слова:** нанокремнезём, хлориды металлов, водные суспензии, распределение частиц по размерам, дзета-потенциал.

*(Received 9 June, 2015)*

## 1. INTRODUCTION

Pyrogenic (fumed) silica (PS200) is widely used as sorbent and carrier in drug delivery (medicine, biotechnologies, *etc.*) due to its physical and chemical properties, such as well-developed surface, chemical inertness, significant adsorption capacity [1–6]. Additionally, it can interact with different biomolecules. For instance, amino acid, bilious acid and proteins depending on the method of application [3–7]. The buffer solution of NaCl ( $C_{\text{NaCl}}=0.9$  wt.%) is often used in various studies of interactions of silica surface with these molecules because sodium chloride is present both in blood plasma and histic liquid of organism (at the concentration of  $C_{\text{NaCl}}=0.9$  wt.%). It is the most important inorganic compound keeping osmotic blood pressure and extracellular liquid [8, 9]. Thus, the investigations of mechanisms of the silica surface interaction with electrolytes in aqueous media are of principal importance and actual at present time.

Electrical double layer (EDL) is the thin surface layer, which consist of separated oppositely charged ionic sites. EDL occurs on interface of two or more different phases. Formation of EDL can significantly affect the rate of electrode processes (i), adsorption of various ions and neutral molecules (ii), dispersion system stability (iii), wettability (iv), and so forth. In biological systems, the formation and destruction processes of the EDL on cellular membranes are associated with the propagation of electrical pulses inside nerve and muscle fibres [10–17].

Zeta potential ( $\zeta$ ) is one of the key parameters of EDL. It is a

physical quantity characterizing the slipping plane. The value of  $\zeta$  is determined by free counterions localized within the diffusion layer. Furthermore,  $\zeta$  enables evaluating electrokinetic phenomena in the interface [10–14], depends on the morphology and nature of silica surface [3]. Both sign (+/–) and magnitude of  $\zeta$  derived from the study of electrokinetic phenomena are used for the characterization of surface electrical properties in the cases of adsorption, adhesion and aggregative stability of colloid systems. Therefore, the value of zeta potential of nanoparticles allows making a conclusion about both of their potential activity and adsorption ability [3, 4, 10–14].

EDL can be described in terms of proton-donor parameters of silica surface, such as a dissociation constant ( $pK_a$ ) of silanol sites in the presence of electrolytes. For accurate grasp of the silanol-sites' ionization mechanisms and impact of a variety of salts, it is necessary to study processes at the molecular level. The information can be obtained with quantum-chemical calculations of spatial and electronic structure of certain molecular models corresponding to the adsorption complex of a hydrated ion on the fumed silica surface. Thus, the influence of the hydrated chloride alkaline metal ions upon the structure and protolytic properties of silanol sites is modelled here.

## 2. EXPERIMENTAL SECTION

### 2.1. Materials

Pyrogenic (fumed silica (nanosilica) PS200 (pilot plant at the Institute of Surface Chemistry, Kalush, Ukraine; 99.8% purity) has the specific surface area  $S_{BET} = 232 \text{ m}^2/\text{g}$  corresponding to the average radius of primary nanoparticles  $a_{av} = 3000/(\rho_0 S_{BET}) \approx 5.88 \text{ nm}$ , where  $\rho_0$  is the density of fumed silica ( $\rho_0 \approx 2.2 \text{ g/cm}^3$ ).

### 2.2. Experimental Setup

Electrophoretic mobility and particle size distribution (PSD) investigations were performed using a Zetasizer 3000 or a Zetasizer Nano ZS (Malvern Instruments) apparatus using a universal dip cell (ZEN1002) and a disposable polystyrene cell (DTS0012) for zeta potential measurements [4, 18]. Distilled water with certain amounts of dissolved salt (0.001–0.1 M LiCl, NaCl, KCl) and nanosilica PS200 (5–50 g per 1 dm<sup>3</sup> of aqueous solution of a salt) were utilized to prepare suspensions sonicated for 2 min using an ultrasonic disperser (Sonicator Misonix; 500 W power, 22 kHz frequency). The suspensions were equilibrated for 24 h.

According to the Smoluchowski theory [12–17], there is a linear relationship between the electrophoretic mobility  $U_e$  and the  $\zeta$  potential:

$$U_e = \zeta, \quad (1)$$

where  $\zeta$  is a constant for a thin EDL at  $\kappa a \gg 1$  (where  $a$  denotes the particle radius, and  $\kappa$  is the Debye–Hückel parameter). For a thick EDL ( $\kappa a < 1$ ), *e.g.*, at pH close to the isoelectric point (IEP), the equation with the Henry correction factor is more appropriate:

$$U_e = 2\varepsilon\zeta/(3\eta), \quad (2)$$

where  $\varepsilon$  is the dielectric permittivity; and  $\eta$  is the viscosity of the liquid [10–17]. Numerical values of  $\varepsilon$  and  $\eta$  are set during the measure.

Ohshima obtained a general mobility expression for a swarm of identical spherical colloidal particles in the concentrated suspensions [16, 17], which gives the results close to Eq. (1) at  $\kappa a > 100$  (this is typical for other theories of electrophoresis more exact than the Smoluchowski theory; *i.e.*, under this condition, the Smoluchowski equation is well suited and, therefore, widely utilized, but strongly differ at  $\kappa a < 10$  [3, 4, 19–23]).

The photon correlation spectroscopy (PCS) is a powerful physical method successfully applied to solve various problems in many technological and scientific branches such as colloidal chemistry, biochemistry, biophysics, molecular biology, food technology, *etc.* PCS is based on measurement of spectral characteristics of induced monochromatic coherent light after passing it through liquid with possibility of particles registration due to the Doppler effect. The hydrodynamic diameter (or effective diameter,  $D_{\text{ef}}$ ) of particles can be 10–15% more than geometrical one [4], and it also can get varied in range from 2.0 to 10000.0 nm.

An average size value can be estimated in respect to the intensity:

$$D_{\text{ef}} = \sum_i N_i d_i^6 / \sum_i N_i d_i^5, \quad (3)$$

and particle volume (or weight):

$$d_v = \sum_i N_i d_i^4 / \sum_i N_i d_i^3, \quad (4)$$

where  $d_i$  and  $N_i$  are diameter and number of  $i$ -th particles, respectively [3, 4, 23].

The quantum-chemical calculations of spatial and electronic

structures of the molecular models attributed to the adsorption complex of hydrated salt ions on the fumed silica surface were performed by means of the theory electron density functional in combination with the exchange–correlation functional B3LYP and split valence basis set 6-31++G(*d*, *p*). The influence of aqueous medium was taken into consideration involving the model of solvent SMD (CPCM). As the model of silica surface was chosen the Si<sub>8</sub>O<sub>12</sub>(OH)<sub>8</sub> cluster (Figs. 3–5). All calculations were made via the US GAMESS program packages. The methods of the calculation are described in detail in [24].

The Gibbs free energy of reaction ( $\Delta G_{\text{reac}}$ ) of acid dissociation of silica surface silanol sites at 298 K was calculated according to the equation (5) [25–27]:

$$\Delta G_{\text{reac}} = \Delta G_{\text{trans}} + \Delta G_{\text{rot}} + \Delta G_{\text{vib}}; \quad (5)$$

in this formula,  $\Delta G_{\text{reac}} = G^0_{298}(\text{products of reaction}) - G^0_{298}(\text{reactants})$ ,  $G^0_{298} = E_{\text{tot}} + \text{ZPE} + G_{0 \rightarrow 298 \text{ K}}$ , and  $E_{\text{tot}}$  is the full energy of corresponding optimized structure, energy of zero-point oscillations (ZPE) and the value adjustments  $G_{0 \rightarrow 298 \text{ K}}$ . The values above were obtained by diagonalization of the Gauss matrixes of reaction products and reagents. Within the fixed rotor and harmonic oscillator approximation, these values were determined as the sum of the contributions of translational, rotational and vibrational motions at design temperature. The interaction of vibrational and rotational degrees of freedom was neglected.

Acid dissociation constant ( $\text{p}K_a$ ) is connected with the Gibbs energy ( $\Delta G_{\text{reac}}$ ) of reaction  $\text{SiOH} \rightleftharpoons \text{SiO}^- + \text{H}^+$  according to the equation:

$$\text{p}K_a = \Delta G_{\text{reac}} / (2.303RT), \quad (6)$$

where  $R$  is universal gas constant and  $T$  is absolute temperature.

### 3. RESULTS AND DISCUSSION

#### 3.1. Results

The investigations of PS200 aqueous suspensions at concentrations of solid phase from 0.5 wt.% to 5 wt.% (in absence of any indifferent electrolytes [10, 11]) indicate negative values of zeta potential which are changed *vs.* increase of solid phase concentration in the range from –30 to –10 mV, respectively (Fig. 1, *a*). It can be attributed to the presence of ionogenic hydroxyl sites on the silica surface. It is precisely the surface density of ionized sites that is

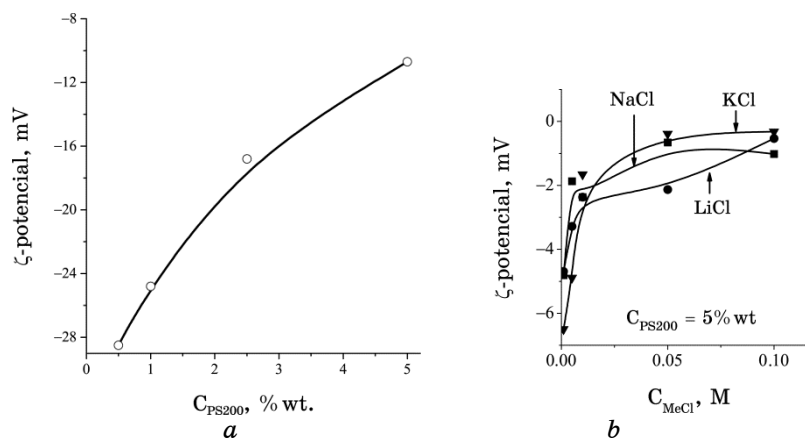


**Fig. 1.** Zeta potential as a function of PS200 concentration in electrolyte-free aqueous suspension (a) and in the presence of electrolytes (b): ●—LiCl, ■—NaCl, or ▼—KCl (in solution at  $C_{PS200} = 5$  wt.%).

responsible for specific silica-surfaces' charge.

Addition of alkaline metal chlorides into the silica suspension strongly affects influences the zeta potential of  $SiO_2$ -water-MeCl system. A growth of the salt concentration is accompanied by a decrease in the negative value of the zeta potential toward zero (Fig. 1, b). This can be caused by the adsorption of metal cations onto the silica surface or their distribution in the EDL near the slipping plane at the highest concentration of nanosilica (5 wt.%).

The effect of cation  $K^+$  on  $\zeta$ -potential is stronger than that of  $Li^+$  and  $Na^+$  (Fig. 1, b). This is due the increase of ion exchange efficiency with increasing cation radius according to the well-known lyotropic series ( $Li^+ < Na^+ < K^+$ ) [10–15].

These ions are more inclined to polarization and exhibit a marked ability to be attracted toward oppositely charged surface. Moreover, there are the bigger radius of the ion and the less radius of its hydration shell at the constant charge. The presence of that hydrated sheath reduces the electrostatic interaction between cations and particles surface preventing adsorption of the ions.

The PSD demonstrate the formation of primary silica nanoparticles ( $\sim 10$  nm), their aggregates ( $30 \text{ nm} \leq d_v \leq 1 \mu\text{m}$ ) and agglomerates ( $d_v > 1 \mu\text{m}$ ) with the main contribution of aggregate (Fig. 2) [2, 23]. Bi- and trimodal size distribution of silica particles in aqueous suspension without addition of any electrolyte is observed (Fig. 2, a). It is obvious that there are individual primary particles (16 nm), their aggregates and agglomerates thereof (300–1000 nm) also formed.

Aggregation degree of nanosilica particles depends on both the

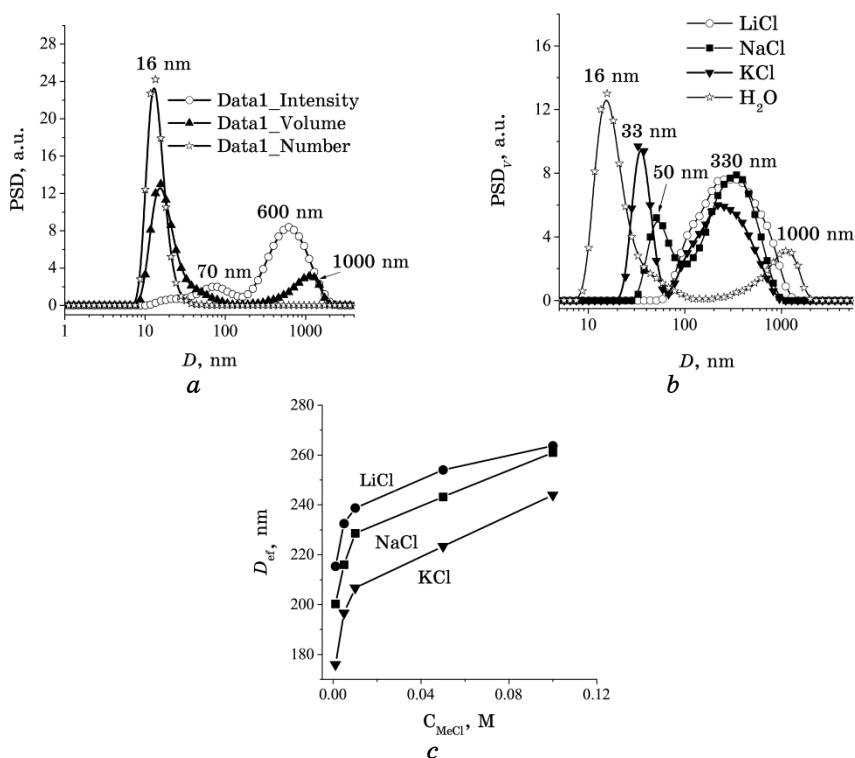


**Fig. 2.** Particle size distributions with respect to: (a) the light scattering intensity, particles volume and number at  $C_{PS200} = 5$  wt.% in electrolyte-free aqueous suspension; (b) the particle volume at  $C_{PS200} = 5$  wt.% and  $C_{MeCl} = 0.01$  M; (c) effective diameter of particles (determined from the light scattering intensity) as a function of the salt content (0.001–0.1 M) for LiCl, NaCl, and KCl at  $C_{PS200} = 5$  wt.% in the suspensions.

dispersion media and particle characteristics—particles' size distribution and pH, which influences degree of dissociation of surface silanols, *i.e.*, affects the surface charge density. In fact, chemical bonds between particles of PS200 found in aggregates are absent. Mainly, the interactions are provoked by the van der Waals attraction and electrostatic repulsion [3, 23]. Electrolyte addition into the SiO<sub>2</sub>–water system results in irregular charge distribution (1) and change of EDL thickness (2) in contradistinction from those of salt-free SiO<sub>2</sub>–water. It makes an impact on the interaction between silica nanoparticles.

The addition of alkaline metal chlorides leads to significant changes in nanosilica particles distribution in the SiO<sub>2</sub>–water–MeCl system and causes the aggregation of primary PS200 particles (Fig. 2, b). The size of the aggregates considerably depends on the cation

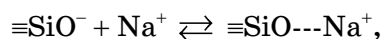
character.  $\text{Li}^+$  cation is the largest in line  $R(\text{Li}^+) > R(\text{Na}^+) > R(\text{K}^+)$ . Hence, the aggregates of size less than 330 nm do not exist in the presence of more hydrated  $\text{Li}^+$  cations (Fig. 2, *b*). The diminution of cation hydrated radius leads to two phenomena: (i) conversion in the PSD from monomodal (LiCl)-to-bimodal (NaCl, KCl) distribution profiles; (ii) addition of NaCl, KCl result in aggregates size changing vs. cation hydrated radius: 50 nm for  $R(\text{Na}^+)$  and 33 nm for  $R(\text{K}^+)$  (Fig. 2, *b*).

It is worth noting that the salt addition into  $\text{SiO}_2$ -water system causes destruction of large aggregates (of about 1  $\mu\text{m}$ ), which are observed in this system without any electrolytes and formation of stable PS200 aggregates (of 330 nm) (Fig. 2, *b*).

The conversion of MeCl concentration from 0.001 to 0.1 M in the  $\text{SiO}_2$ -water-MeCl system leads to the diminution of the average effective diameter ( $D_{\text{ef}}$ ) of nanosilica particles down to 180–270 nm. (Fig. 2, *c*). The maximal value of  $D_{\text{ef}}$  at  $C_{\text{MeCl}} = 0.1$  M is observed. The values of the average effective diameter of nanosilica aggregates are increased with cation hydrated radius in the order  $R(\text{Li}^+) > R(\text{Na}^+) > R(\text{K}^+)$  (at  $C_{\text{MeCl}} = \text{const}$ ; Fig. 2, *c*).

### 3.2. Quantum-Chemical Calculations

Modelling the structure of the hydration shells of alkaline earth chlorides and chlorine anion were found that  $\text{Li}^+$  cation is surrounded with water molecules ( $n \geq 4$ ) in the first hydration shell. However, surrounding of  $\text{Na}^+$  and  $\text{K}^+$  cations is characterized by higher amount of  $\text{H}_2\text{O}$  molecules ( $n \geq 6$ ). Previously, the dissociation of silanol groups without any electrolyte was discussed in [24]. Since cations of alkaline metal chlorides can interact with non-dissociated (similar contacts are present in the crystal structure of sodium hydrosilicates) as well as with deprotonated silanols according to the scheme:



it is essential to consider both cases in order to compute the dissociation constant value and its change in the presence of electrolyte ions. Thus, as a result of the calculation, true values of the dissociation constants will not be obtained, but they may be apparent. The difference between these results is caused by polarization effect of electrolyte ions. By means of this one, the change in ionic strength in the electrolyte solution is reflected.

Figure 3 shows the equilibrium complex structure consisting of  $\text{Li}^+$ ,  $\text{Cl}^-$ , nine water molecules and silica cluster with eight silicon-oxygen tetrahedra.



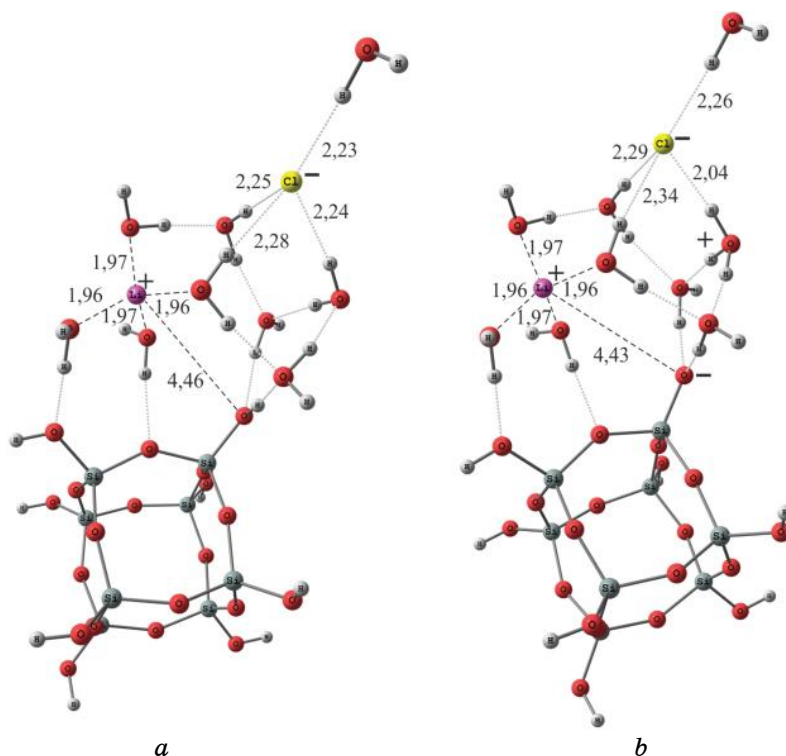


**Fig. 3.** The equilibrium complex structure containing  $\text{Si}_8\text{O}_8(\text{OH})_8$  cluster, nine water molecules, and  $\text{Li}^+\text{Cl}^-$  ion pair: (a) molecular state, (b) dissociated silanol state. The bond lengths are expressed in  $\text{\AA}$ .

The distance between  $\text{Li}^+$  cation and oxygen atom of non-dissociated silanol group is  $4.46 \text{ \AA}$  (Fig. 3, a), and in the case of the deprotonated silanol group, it is equal to  $4.43 \text{ \AA}$  (Fig. 3, b). The length of the bond between  $\text{Li}^+$  cation and O atom of water molecule in the first hydration shell is  $1.96\text{--}1.97 \text{ \AA}$  (Fig. 3). This result supports the suggestion that oxygen atom of silanols does not enter the coordination sphere of  $\text{Li}^+$  cation. This can be explained by  $\text{Li}^+$  cations ability to coordinate a water molecule, which the presence prevents the formation of bonds between  $\text{Li}^+$  cation and oxygen atom of Si-OH group on the nanosilica particle surface. Hence,  $\text{Li}^+$  cation interacts with active centres of nanosilica surface (Si-OH) by water molecules from its hydration shell, in other words, by way of electrostatic mechanism. Unlike complex having  $\text{Li}^+$  and  $\text{Cl}^-$  ions, the distances between  $\text{Na}^+$  cation and oxygen atom in non-dissociated (Fig. 4, a) and deprotonated (Fig. 4, b) silanols in the complex with hydrated  $\text{Na}^+$  and  $\text{Cl}^-$  ions are  $2.50 \text{ \AA}$  and  $2.36 \text{ \AA}$ , respectively. It should be noticed the distance between  $\text{Li}^+$ ,  $\text{Na}^+$  cations and oxygen

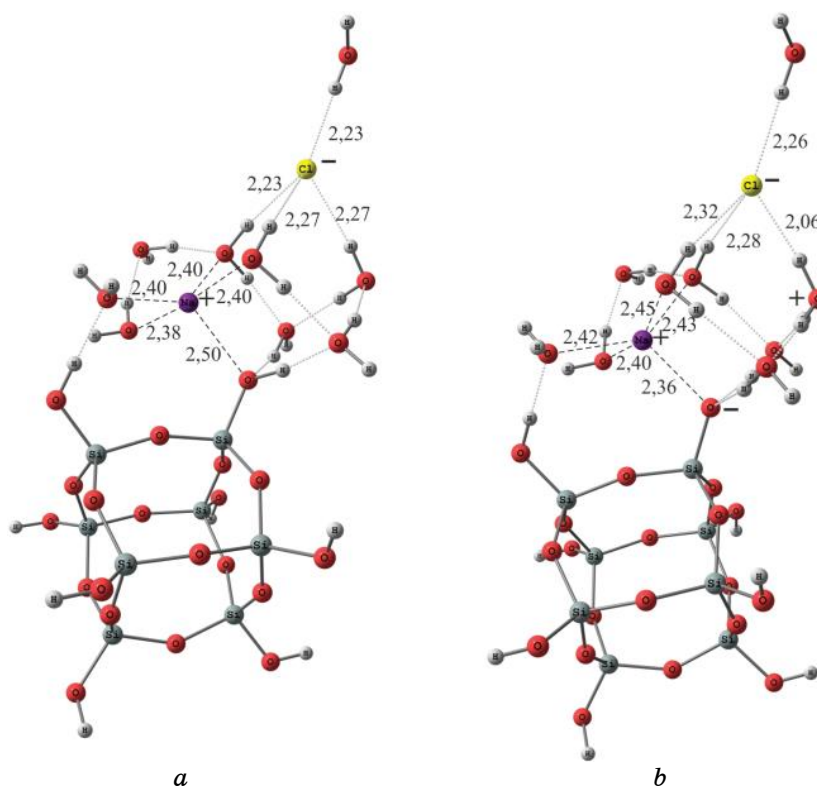
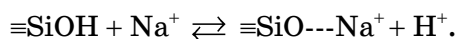


Fig. 4. The equilibrium complex structure containing  $\text{Si}_8\text{O}_8(\text{OH})_8$  cluster, nine water molecules, and  $\text{Na}^+\text{Cl}^-$  ion pair: (a) molecular state, (b) dissociated silanol state. The bond lengths are expressed in  $\text{\AA}$ .

atom of non-dissociated silanol is larger than that between cation and oxygen atom of water molecule in the first hydrated shell ( $2.42 \pm 0.02 \text{\AA}$ ). It points to the fact of incorporation of silanol oxygen atom into the coordinating sphere of  $\text{Na}^+$  cation.

This process is accompanied by the dissociation of silanol sites at high pH values (more than 7) according to the scheme:



A similar dependence for complexes having hydrated cations  $\text{K}^+$  and  $\text{Cl}^-$  (Fig. 5) is observed. The distance  $\text{K}^+ \cdots \text{O}(\text{H})-\text{Si}\equiv$  is  $2.96 \text{\AA}$  (Fig. 5, a). The distance from  $\text{K}^+ \cdots \text{O}^--\text{Si}\equiv$  is  $2.81 \text{\AA}$  (Fig. 5, b). Since the distance between cation and oxygen atom of water molecule in the first hydrated shell is  $2.80 \pm 0.04 \text{\AA}$ , we are able to confirm that silanol oxygen atom has to do with the first coordinating sphere of this cation.

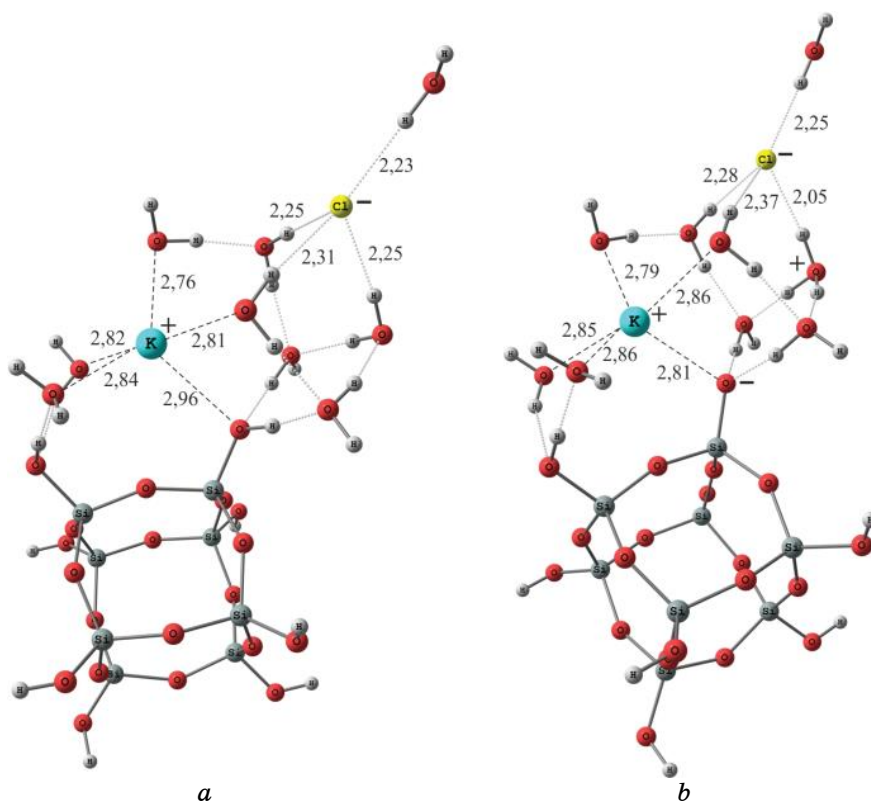


**Fig. 5.** The equilibrium complex structure containing  $\text{Si}_8\text{O}_8(\text{OH})_8$  cluster, nine water molecules, and  $\text{K}^+\text{Cl}^-$  ion pair: (a) molecular state, (b) dissociated silanol state. The bond lengths are expressed in  $\text{\AA}$ .

Calculated values of dissociation constants of cluster silanols  $\text{Si}_8\text{O}_{12}(\text{OH})_8$  in the presence of hydrated ions of alkaline chloride metal are shown in the Table (nine water molecules were taken into consideration too). The obtained values of apparent  $\text{p}K_a$  are functions of chemical character of cations ( $\text{Li}^+ > \text{Na}^+ > \text{K}^+$ ). This gives

**TABLE.** The Gibbs free-energy change ( $\Delta G_{\text{reac}}$ ) of deprotonation, and dissociation constant ( $\text{p}K_a$ ) of silanol of  $\text{Si}_8\text{O}_{12}(\text{OH})_8$  cluster under the interaction with hydrated complexes of LiCl, NaCl, KCl.

Complex	$\Delta G_{\text{reac}}$ , kJ/mole	$\text{p}K_a$
$\text{LiCl} + 9\text{H}_2\text{O} + \text{Si}_8\text{O}_{12}(\text{OH})_8$	39.76	6.97
$\text{NaCl} + 9\text{H}_2\text{O} + \text{Si}_8\text{O}_{12}(\text{OH})_8$	35.65	6.25
$\text{KCl} + 9\text{H}_2\text{O} + \text{Si}_8\text{O}_{12}(\text{OH})_8$	32.61	5.71

reason to conclude that acidic properties of the silica surface silanol groups are enhanced with increasing of cation radius ( $\text{Li}^+ < \text{Na}^+ < \text{K}^+$ ).

It should be noticed that the values of silica  $\text{p}K_a$  in the presence of alkaline chloride metals correlate with the values of average effective diameter  $D_{\text{ef}}$  at  $C_{\text{MeCl}} = \text{const}$  (Fig. 2, Table).

Thus, the negative charge of silica surface will increase and it results in less degree of aggregation of silica nanoparticles (primary and aggregates) due to the Coulomb repulsion. The measurements of the pH values of aqueous nanosilica suspension were performed in the presence of LiCl, NaCl, KCl (Fig. 6).

The data obtained confirm the increase of negative charge on the silica surface accompanied by changing nature and concentration of electrolyte. Therefore, experimental and quantum-chemical methods provide the results, which give us grounds to expect that the main

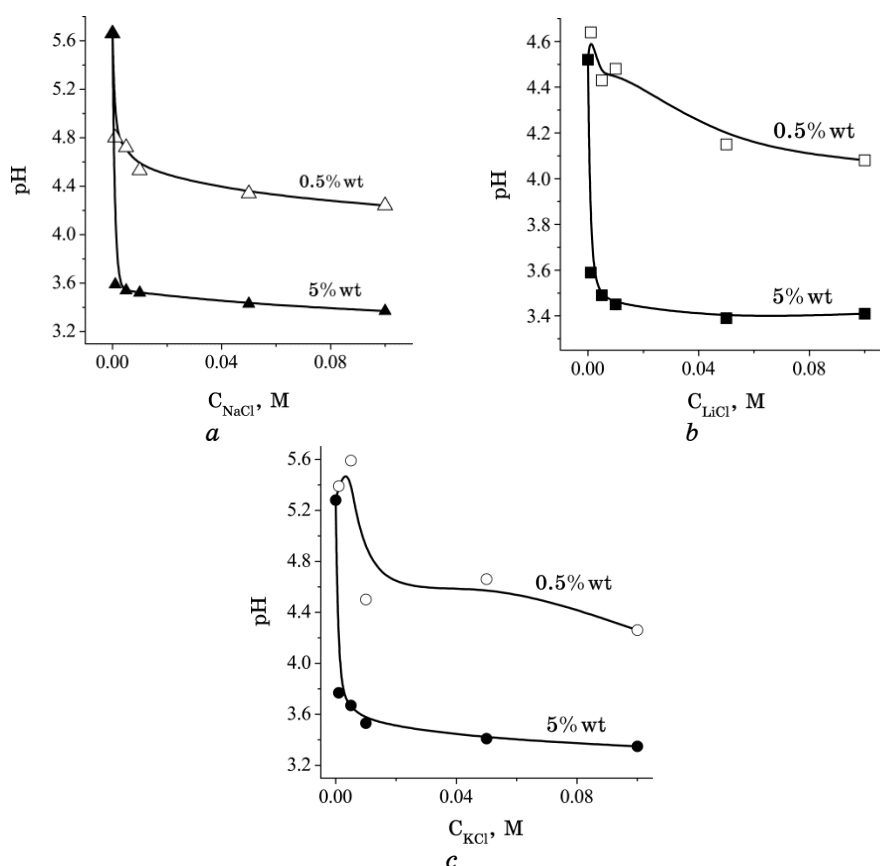


**Fig. 6.** pH as a function of electrolyte concentration ( $\text{MeCl}$ ,  $\text{Me} = \text{Li}^+$ ,  $\text{Na}^+$ ,  $\text{K}^+$ ) at  $C_{\text{PS200}} = 0.5$  and 5 wt.% in the  $\text{SiO}_2$ -water- $\text{MeCl}$  system.

case of electrolyte native influence on aggregation and zeta potential of nanosilica particles in aqueous media is the different effects of  $\text{Li}^+$ ,  $\text{Na}^+$  and  $\text{K}^+$  cations on apparent dissociation constant value of nanosilica surface silanols. Based on the results of this investigation, we can formulate that it is possible to exert control of the activity and sorption capacity of silica nanoparticles by the variation of the electrolyte concentration in the silica suspension. Furthermore, the morphological properties of the particles in an aqueous medium can be also operated by this way.

#### 4. CONCLUSIONS

The results indicate that nanosilica particles distribution, the change of average effective diameter ( $D_{\text{ef}}$ ) of nanosilica particles in the  $\text{SiO}_2$ -water-MeCl system, and electrokinetic behaviour (zeta potential) of suspensions considerably depend on the salt concentration and the types of cations (LiCl, NaCl, KCl). The value of zeta potential has been shown to approach zero with increase of the molar electrolyte concentration to 0.1 M in the case of univalent cations. It should be noted that  $D_{\text{ef}}$  and zeta potential are symbately changed in the order as follows:  $R(\text{Li}^+) > R(\text{Na}^+) > R(\text{K}^+)$ . This is also confirmed with results of quantum-chemical calculations and estimated thermodynamic parameters agreeably to the lyotropic series shown above.

#### REFERENCES

1. *Medical Chemistry and Clinical Application of Silicon Dioxide* (Eds. A. A. Chuiko) (Kiev: Naukova Dumka: 2003) (in Russian).
2. *Surface Chemistry in Biomedical and Environmental Science: NATO Science Series II: Mathematics, Physics and Chemistry. Vol. 228* (Eds. J. P. Blitz and V. M. Gun'ko) (Dordrecht: Springer: 2006)
3. V. M. Gun'ko, V. I. Zarko, R. Leboda, and E. Chibovski, *Adv. Colloid Interface Sci.*, **91**: 1 (2001).
4. V. M. Gun'ko, A. V. Klyueva, Y. N. Levchuk, and R. Leboda, *Adv. Colloid Interface Sci.*, **10**: 201 (2003).
5. N. N. Vlasova and L. P. Golovkova, *Colloid J.*, **66**: 657 (2004).
6. L. A. Belyakova, L. N. Besarab, N. V. Roik et al., *J. Colloid Interface Sci.*, **294**: 11 (2006).
7. V. M. Gun'ko, I. V. Mikhailova, V. I. Zarko et al., *J. Colloid Interface Sci.*, **260**: 56 (2003).
8. J. D. Harley and J. Margolis, *Nature*, **189**: 1010 (1961).
9. B. I. Gerashchenko, V. M. Gun'ko, I. I. Gerashchenko et al., *Cytometry*, **49**, No. 2: 56 (2002).
10. J. Lyklema, *Fundamentals of Interface and Colloid Science* (London: Academic Press.: 1991), vol. **1**.

11. J. Lyklema, *Fundamentals of Interface and Colloid Science* (London: Academic Press.: 1995), vol. 2.
12. R. J. Hunter, *Zeta Potential in Colloid Science: Principles and Application* (London: Academic Press: 1981).
13. R. J. Hunter, *Foundations of Colloid Science* (Oxford: Oxford University Press.: 1989), vol. 1.
14. W. B. Russel, D. A. Saville, and W. R. Schowalter, *Colloidal Dispersions* (Cambridge: Cambridge University Press.: 1992).
15. A. V. Delgado, F. Gonzalez-Caballero, R. J. Hunter et al., *J. Colloid Interface Sci.*, **309**: 194 (2007).
16. H. Ohshima, *J. Colloid Interface Sci.*, **188**: 481 (1997).
17. H. Ohshima, *J. Colloid Interface Sci.*, **195**: 137 (1997).
18. www.malvern.com
19. V. M. Gun'ko, V. I. Zarko, E. F. Voronin et al., *J. Colloid Interface Sci.*, **300**: 20 (2006).
20. V. M. Gun'ko, V. I. Zarko, E. V. Goncharuk et al., *Adv. Colloid Interface Sci.*, **131**, Nos. 1–2: 1 (2007).
21. V. M. Gun'ko, V. I. Zarko, and V. V. Turov, *Powder Technology*, **195**: 245 (2009).
22. V. M. Gun'ko and V. V. Turov, *Nuclear Magnetic Resonance Studies of Interfacial Phenomena* (Boca Raton: CRC Press: 2013).
23. V. M. Gun'ko, L. S. Andriyko, V. I. Zarko et al., *Central European J. Chem.*, **12**: 480 (2014).
24. E. Demianenko, M. Ilchenko, A. Grebenyuk, and V. Lobanov, *Chem. Phys. Lett.*, **515**: 274 (2011).
25. M. W. Schmidt, K. K. Baldridge, J. A. Boatz et al., *J. Comput. Chem.*, **14**: 1347 (1993).
26. R. G. Parr and W. Yang, *Density-Functional Theory of Atoms and Molecules* (Oxford: Oxford Univ. Press: 1989).
27. A. D. Becke, *Phys. Rev. A*, **38**, No. 6: 3098 (1988).